

The Viscosity and Thermal Conductivity Coefficients of Dilute Argon, Krypton, and Xenon

Cite as: Journal of Physical and Chemical Reference Data **2**, 619 (1973); <https://doi.org/10.1063/1.3253128>
Published Online: 29 October 2009

H. J. M. Hanley



[View Online](#)



[Export Citation](#)

ARTICLES YOU MAY BE INTERESTED IN

[Elastic Properties of Metals and Alloys, I. Iron, Nickel, and Iron-Nickel Alloys](#)

Journal of Physical and Chemical Reference Data **2**, 531 (1973); <https://doi.org/10.1063/1.3253127>

[The Viscosity and Thermal Conductivity Coefficients for Dense Gaseous and Liquid Argon, Krypton, Xenon, Nitrogen, and Oxygen](#)

Journal of Physical and Chemical Reference Data **3**, 979 (1974); <https://doi.org/10.1063/1.3253152>

[Measurements of the Viscosity of Krypton](#)

The Journal of Chemical Physics **38**, 1123 (1963); <https://doi.org/10.1063/1.1733813>



Where in the world is AIP Publishing?
Find out where we are exhibiting next

The Viscosity and Thermal Conductivity Coefficients of Dilute Argon, Krypton, and Xenon

H. J. M. Hanley

Cryogenics Division, National Bureau of Standards, Boulder, Colorado 80302

The viscosity and thermal conductivity coefficients of dilute argon, krypton, and xenon are reviewed and tables of recommended values presented. The tables were generated using the appropriate kinetic theory expressions with the $m=6-8$ potential. The temperature range covers from about one-half critical temperature to 2000 K for each gas. A general estimate of the accuracy is one percent increasing to one and three-quarters percent for temperatures above 1000 K.

Key words: Dilute gas; kinetic theory; $m=6-8$ potential function; rare gases; thermal conductivity coefficient; viscosity coefficient.

1. Introduction

In this paper the dilute gas transport properties of the gases argon, krypton, and xenon are discussed and tabulated values of the viscosity and thermal conductivity coefficients presented. The temperature region covered ranges from about one-half critical temperature to 2000 K for each gas.

The tables are based strongly on data which have become available in the last six years or so. On experimental grounds these data are judged to be generally more reliable than corresponding data produced prior to that time. Further, the tables were generated by combining kinetic theory with the data leading to a consistent representation of both the viscosity and thermal conductivity coefficients for a given gas. Moreover, kinetic theory enables one to verify that these coefficients are compatible with other transport properties—the diffusion coefficient and the thermal diffusion factor—and with equilibrium properties via the second virial coefficient.

2. Experimental Methods and Data

Experimental techniques will not be discussed in this paper. Some general references are: viscosity, the article by Bruges and Whitelaw [1]¹ and the references therein, and the older book of Barr [2]; thermal conductivity, the two volumes edited by Tye [3], which contain several articles on experimental techniques and numerous references. Reference should also be made to the books of Golubev on viscosity [4], and of Vargaftik [5] and Tsederberg [6] on thermal conductivity. Discussions on recent experimental procedures include those given by Kestin [7, 8] for viscosity and by McLaughlin [9] for thermal conductivity.

However, there are three remarks:

1. Most of the viscosity data for the common gases have been obtained from one of two procedures known as the capillary flow and oscillating disc methods, respectively. However, prior to about 1968, apparently self-consistent measurements obtained from the former technique tended to differ systematically from cor-

responding measurements obtained from the latter. The discrepancies were most noticeable at temperatures above 400 K.² For this reason, an evaluation of viscosity data was inconclusive. But since about 1968, several authors have re-examined the capillary flow technique [8, 13, 14] and new results have been published [13-17] which are consistent with the results from the oscillating disc. On this basis, the general conclusion is that many of the older capillary flow viscosity data were incorrect; this conclusion is reinforced by studies on the intermolecular potential function [10] and, to a lesser extent, by a re-evaluation of some of the older experiments [18].

2. Most of the methods that measure the thermal conductivity coefficient are based on setting up a steady state condition in the fluid, viz., a constant known heat flux is maintained at one boundary of the initially isothermal fluid and the resultant temperature gradient measured after reaching the steady state. The several techniques which employ the steady state are generally designated the parallel plate, concentric cylinders, and hot wire methods. We refer to reference [3] for discussions on these approaches. However, the drawback to the procedure is that convection (and to a lesser extent radiation) contributions, have to be properly accounted for, which is a very difficult experimental problem. Consequently, many of the sets of thermal conductivity data available for a particular gas disagree by amounts outside the experimental errors quoted by the authors concerned, and even sets from a particular author are often not internally consistent. In short, on experimental grounds, we are presently unable to set the reliability of the majority of thermal conductivity data at less than five percent.³

¹ Numbers in brackets refer to the references.

Copyright © 1973 by the U.S. Secretary of Commerce on behalf of the United States. This copyright will be assigned to the American Institute of Physics and the American Chemical Society, to whom all requests regarding reproduction should be addressed.

² For example, we compared [10] the capillary flow viscosities of Trant and co-workers [11], with equivalent oscillating disc data from Kestin [12b] and concluded that the viscosity coefficients could differ by as much as ten percent at 2000 K.

³ Several papers have recently been published which describe a non-stationary state (transient) method. For example, see the work of Mani and Vernart [19], Haarman [20], Davis, et al. [21], and McLaughlin and Pittman [9]. These authors discuss the determination of the thermal conductivity coefficient by measuring the temperature rise in a thin suspended wire from the time a current is passed through the wire. The concept is not new but the recent advances result from modern technology which, in particular, allows for the accurate measurement of a small temperature rise within a fraction of a second after the heating current is applied. It seems the transient hot wire technique is capable of giving accurate results although only Haarman [20] has given results of direct relevance to this paper.

3. It will be shown in section 3 that kinetic theory gives a very simple relation between the viscosity and thermal conductivity coefficients of a dilute monatomic gas: given the viscosity coefficient one can calculate the thermal conductivity coefficient directly. For this reason, thermal conductivity data are not required as primary input but are needed only to check on the consistency of the correlating procedure.

In view of the above remarks, our correlation is based on the viscosity data and strongly weighted to favor the viscosity results published since about 1968. A concerted attempt was made to estimate accuracy and reliability of the data from an objective evaluation of the experimental papers helped by discussions with the authors and observations of the apparatus for as many sources as possible. References for the measurements selected are listed in table 1.⁴ General lists of experimental sources are given in references [30–32].

Thermal conductivity references are also presented in table 1. As remarked above, it is not possible to be as selective on experimental grounds with the thermal conductivity data as one could like. The data from references [20], [26], and [37] are judged to be the most reliable but we have no strong reason to exclude any of the data from the other references listed. Other experimental references can be found in references [30], [31], and [50].

3. Kinetic Theory Equations

The Dilute Gas: A dilute gas is a gas whose physical properties can be completely described in terms of uncorrelated binary collisions between its molecules; three body or higher order collisions do not contribute to its properties. One characteristic of a dilute gas is that the viscosity and thermal conductivity coefficients are independent of density or pressure.

The kinetic theory equation for the viscosity of a dilute gas is, to a second approximation [51]:

$$\eta = \frac{5}{16} \frac{(\pi m k T)^{1/2}}{\pi \sigma^2 \Omega^{(2,2)*}} f_\eta, \quad (1)$$

where

$$f_\eta = 1 + \frac{3}{196} \left(8 \frac{\Omega^{(2,3)*}}{\Omega^{(2,2)*}} - 7 \right)^2. \quad (2)$$

Here T is the temperature in kelvin, and the quantities $\Omega^{(l,s)*}$ (in general; $l, s = 1, 2, 3$) are dimensionless collision integrals which take into account the dynamics of a binary collision and are characteristic of the intermolecular potential of the colliding molecules. For a given potential, $\Phi(r)$, with an energy parameter ϵ (defined as the value of $\Phi(r)$ at the maximum energy of attraction) $\Omega^{(l,s)*}$ can be determined as a function of reduced temperature T^*

⁴ Tables have been placed at the end of this paper.

$$T^* = T/(\epsilon/k). \quad (3)$$

The parameter σ is a distance parameter, also characteristic of the intermolecular potential given by $\Phi(\sigma)=0$.

The specific relationship between $\Omega^{(l,s)*}$ and $\Phi(r)$ is as follows. A parameter g^* is defined as the reduced relative kinetic energy of two colliding molecules: $g^{*2} = 1/2 (\mu g^2/\epsilon)$, where μ is the reduced mass, and g the relative velocity. A parameter b is defined as the distance of one molecule from the direction of approach of another before collision.

With r the intermolecular separation and r_c the distance when the molecules are closest, we can show that the angle of scatter, χ , after a collision is related to the potential by

$$\chi = \pi - 2b^* \int_{r_c^*}^{\infty} dr^*/r^{*2} \left[1 - \frac{b^{*2}}{r^{*2}} - \frac{\Phi^*}{g^{*2}} \right]^{-1/2}, \quad (4)$$

where the variables are reduced according to the relations: $b^* = b/\sigma$, $r^* = r/\sigma$, $r_c^* = r_c/\sigma$, $\Phi^* = \Phi/\epsilon$. Integration of χ over all values of b^* produces the cross section, Q^* ,

$$Q^{(l)*} = \frac{2}{\left[1 - \frac{1}{2} \frac{(-1)^l}{1+e} \right]} \int_0^{\infty} (1 - \cos l\chi) b^* db^*. \quad (5)$$

($Q^{(l)*}$ is dimensionless and has been reduced by the corresponding value for molecules interacting with a hard sphere potential.) Finally, $\Omega^{(2,2)*}$ is obtained by integration of Q over all values of g^* ,

$$\Omega^{(l,s)*}(T^*) = \frac{2}{(s+1)!} \frac{1}{T^{*(s+2)}} \int_0^{\infty} \exp(-g^{*2}/T^*) g^{*(2s+3)} Q^{(l)*}(g^*) dg^*. \quad (6)$$

For a dilute monatomic gas, the thermal conductivity coefficient is related to the viscosity by the expression

$$\lambda = \frac{15}{4} \frac{k}{m} \eta f_\lambda / f_\eta \quad (7)$$

where

$$f_\lambda = 1 + \frac{1}{42} \left(8 \frac{\Omega^{(2,3)*}}{\Omega^{(2,2)*}} - 7 \right)^2 \quad (8)$$

For the purposes of this paper we do not have to discuss how equations (1) and (7) were derived or the necessary background assumptions [52].

3.1. Calculation Procedure

Correct use of equations (1) and (7) resolves into the problem of properly selecting a model for the intermolecular potential function for insertion into the collision integral expressions via equation (4). Hanley and Klein have discussed such a selection process [53]

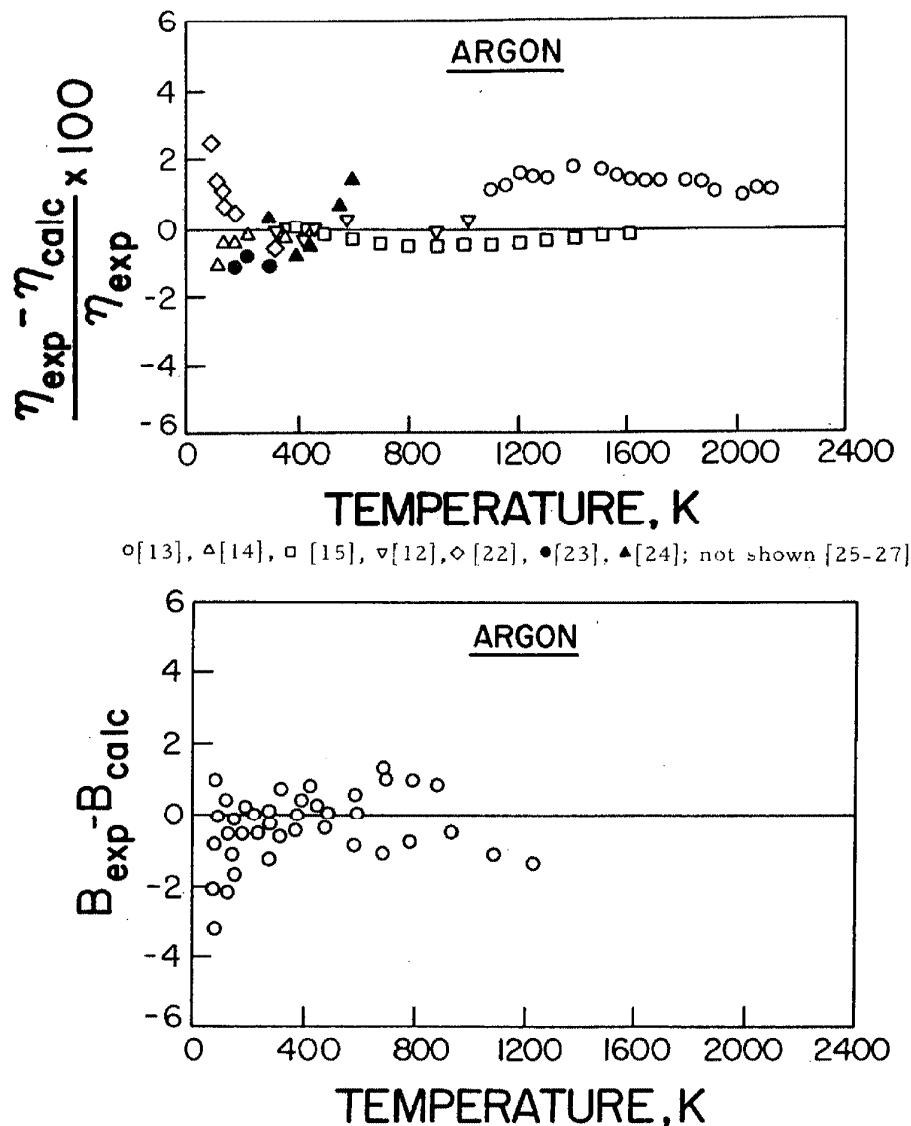


FIGURE 1. Top drawing: percentage deviation plot between experimental dilute gas viscosity coefficients for argon and values calculated from equation (1) with the $m=6-8$ potential: $m=11$, $\gamma=3.0$, $\sigma=3.297$ Å and $\epsilon/k=152.8$ K.
 Bottom drawing: Deviations between the virial coefficients of argon [57] in cm^3/mol compared to values from equation (9) using the same $m=6-8$ parameters.

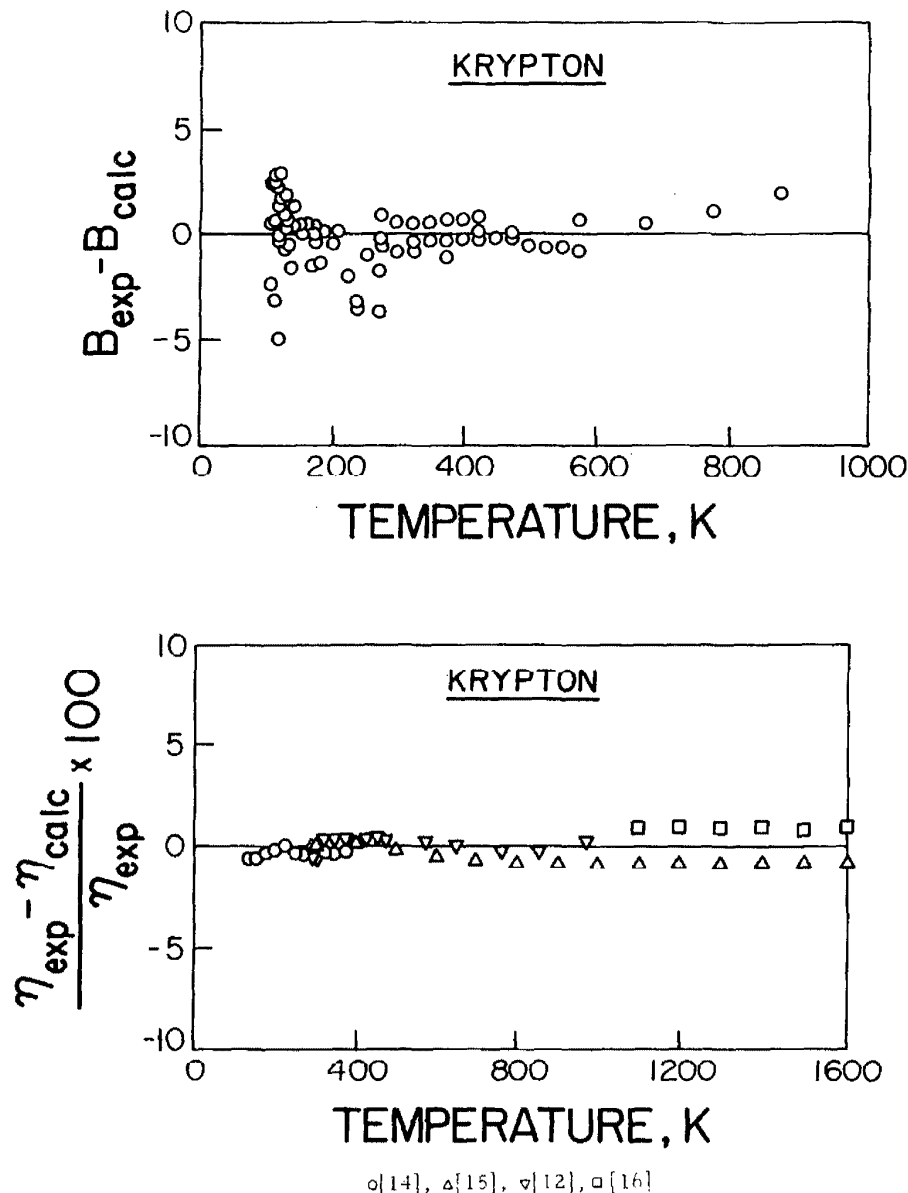
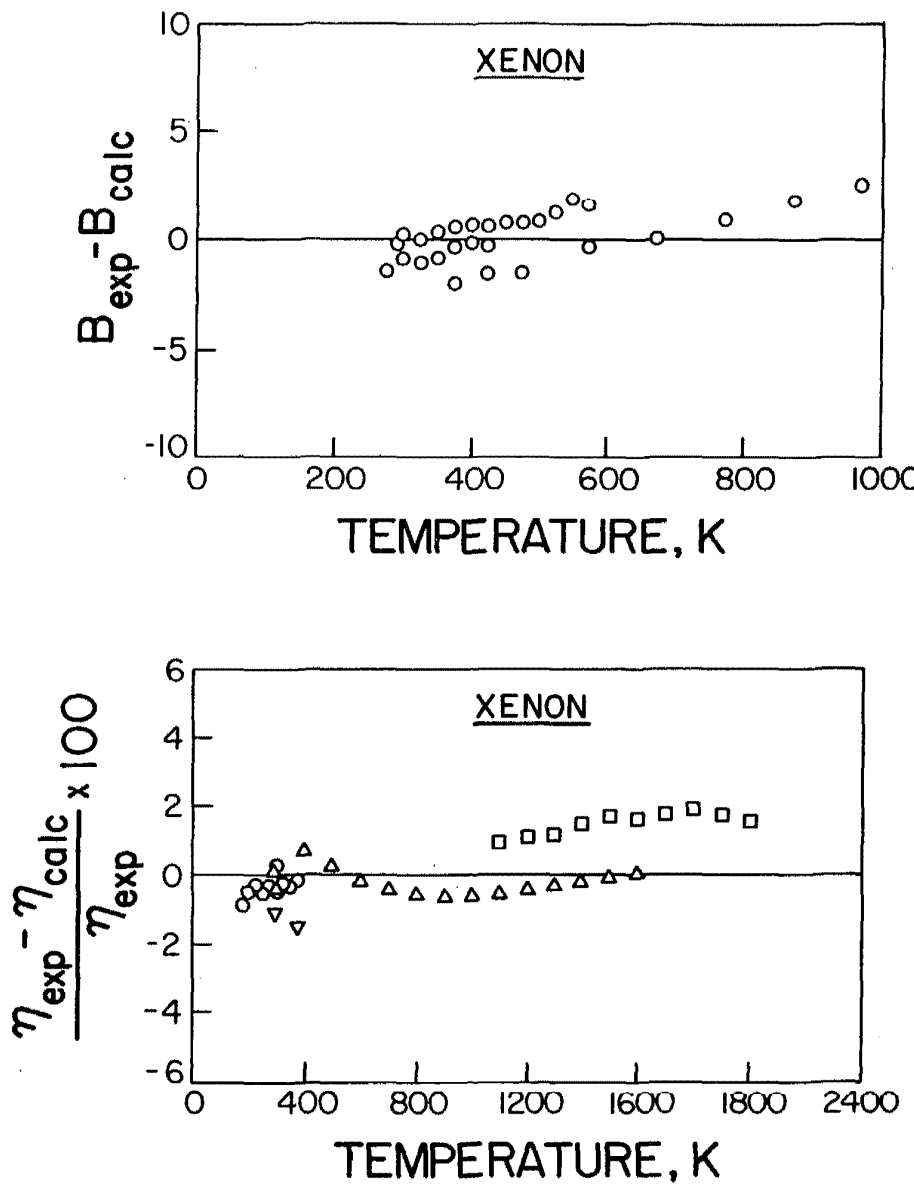


FIGURE 2. Deviation curves for the viscosity and second virial coefficients of krypton. Theoretical values determined for equations (1) and (9) with the $m-6-R$ potential, parameters as given in table 2.



○[14], △[15], □[17], ▽[28, 29]

FIGURE 3. Deviation curves for the viscosity and second virial coefficients of xenon. See table 2.

and various models have been compared and contrasted (for example, see reference [54]). A particular model, called the $m\text{-}6\text{-}8$, was proposed [55] and shown to be successful and practical when used to relate statistical mechanical expressions, such as equations (1) and (7), with experiment. In this paper, we will calculate the dilute gas transport properties with the $m\text{-}6\text{-}8$ potential.

The $m\text{-}6\text{-}8$ potential has the form:

$$\Phi^* = \frac{1}{m-6} [6 + 2\gamma] \left(\frac{d}{r^*}\right)^m - \frac{1}{m-6} [m - \gamma(m-8)] \left(\frac{d}{r^*}\right)^6 - \gamma \left(\frac{d}{r^*}\right)^8, \quad (9)$$

where $d=r_m/\sigma$ with $\Phi(r_m)=-\epsilon$ (or $d\Phi(r_m)/dr=0$). m and γ are parameters representing the repulsion and the attraction due to a $1/r^8$ term, respectively. In reference [55] we have described in detail how the parameters m , γ , σ (or r_m), and ϵ of equation (8) are determined for a given fluid. Essentially, the viscosity and second virial coefficients (B) in the low temperature region (defined as temperatures for which $T^* \leq 2$) are fitted simultaneously to equation (1) and to the equivalent statistical mechanical expression for B :

$$B = \frac{2}{3} \pi N \sigma^3 \int_0^\infty r^{*3} \frac{d\Phi^*}{dr^*} \exp[-\Phi^*/T^*] dr^*, \quad (9)$$

or

$$B = \frac{2}{3} \pi N \sigma^3 B^*(T^*), \quad (9a)$$

where N is Avagadro's number. Tables of $\Omega^{(2,2)*}$ and B^* for several values of m and γ have been published in reference [56]. We have discussed the selection of the viscosity data in section 2. Second virial data were selected carefully by Klein and Levelt Sengers [57].

Parameters obtained from this simultaneous fit were checked by fitting the viscosity coefficient over a wide temperature range. Clearly, if the data are reliable and the potential function sufficiently flexible, the parameters required for a wide temperature range fit of the viscosity coefficient should be those found from the simultaneous fit. This was the case for argon, krypton, and xenon. Parameters for these gases are listed in table 2. Collision integrals and second virial coefficients presented in reference [56] are reproduced here in an appendix.

Having a potential which can properly calculate the viscosity from equation (1), the thermal conductivity coefficient follows from equation (7).

4. Results and Discussion

Tables for the viscosity and thermal conductivity coefficients for argon, krypton, and xenon were gener-

ated from equations (1) and (7) as a function of temperature and presented as tables 3 to 5. Figures 1 to 3 show deviation plots between the selected viscosity data and corresponding tabulated values together with second virial difference plots between experiment and values calculated from equation (9).

In our opinion a proper correlation of the viscosity coefficient has been achieved: the only feature shown in the curves which is not satisfactory is that the two sets of high temperature viscosity data—due to Smith and co-workers and to Guevara and co-workers—differ systematically by about one and three quarters percent. This difference cannot be properly accounted for by using an identical reference viscosity. We cannot prefer one set over the other on experimental grounds but our correlation tends to favor the Smith data. It should be recalled that the high temperature viscosity correlation is largely based on a correlation of low temperature viscosity data and the second virial coefficient. The low temperature correlation gives a potential function, and the high temperature data were used to check on the parameters selected.

Figures 4 to 6 illustrate the deviations between our calculations and experiment for the thermal conductivity coefficient. Considering the scatter in the data, ascribed to experimental problems (section 2), the curves are satisfactory and reinforce the opinion that our correlation procedure is sound. As discussed, thermal conductivity data played no role in the parameter selection of the potential function.

4.1. Accuracy Assessment

In general there are two ways by which one can assess the accuracy of the tabulated values:

1. From *experimental* arguments, that is by attempting to judge the accuracy of the data on which the tables are based by evaluating the experimental procedures, by checking the internal consistency of the data resulting from a particular experiment, and by intercomparing equivalent data obtained from different authors, giving special weight to comparisons between results from different techniques.
2. From *semi-theoretical* arguments, that is by examining how well the potential required to generate the viscosity and thermal conductivity coefficients can represent independent properties, given the appropriate statistical mechanical expressions. If the potential is satisfactory in this context, one can conclude that the transport tables are consistent with other properties and that serious systematic errors are most likely absent. It would be improbable that any systematic errors in the data for different properties, together with the inexactness of the potential model, would fortuitously cancel.

To discuss the first approach: such arguments are basic to the correlation procedure and have been already invoked since our correlation is based on *selected* data (section 2). However, in section 3 and above in this section, it was pointed out that the correlations were especially dependent on a proper fit of viscosity data at

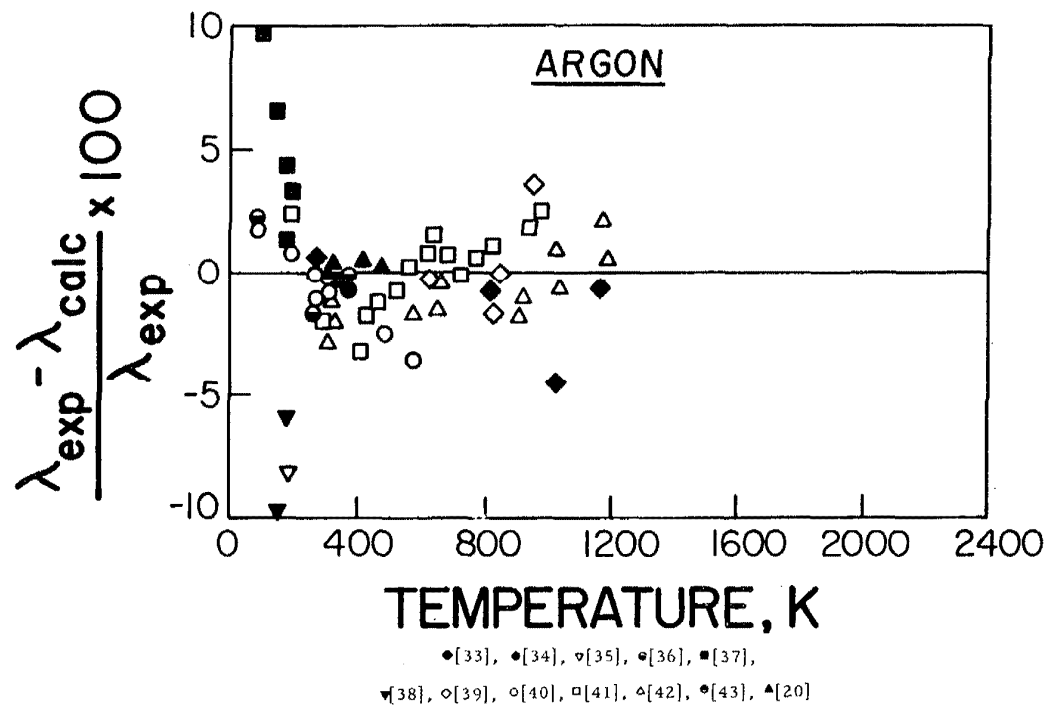


FIGURE 4. Percentage deviation plot of experimental dilute gas thermal conductivity coefficients for argon compared to equation (7) with the $m=6-8$ potential.

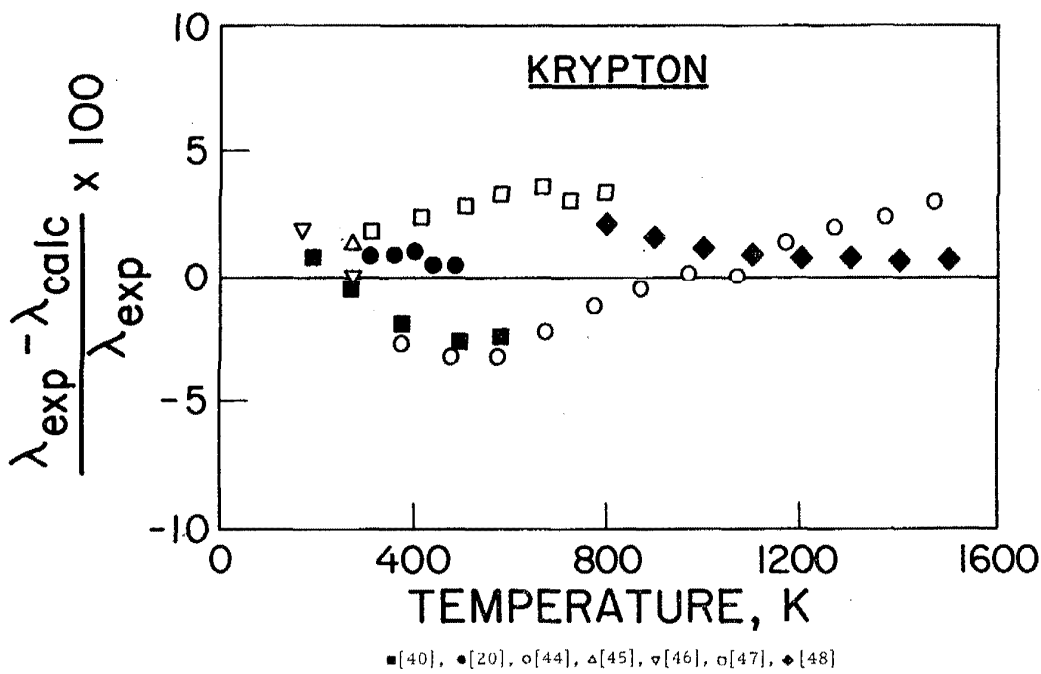


FIGURE 5. Deviation curve for the thermal conductivity of krypton. Theoretical values calculated from equation (7) with parameters given in table 2.

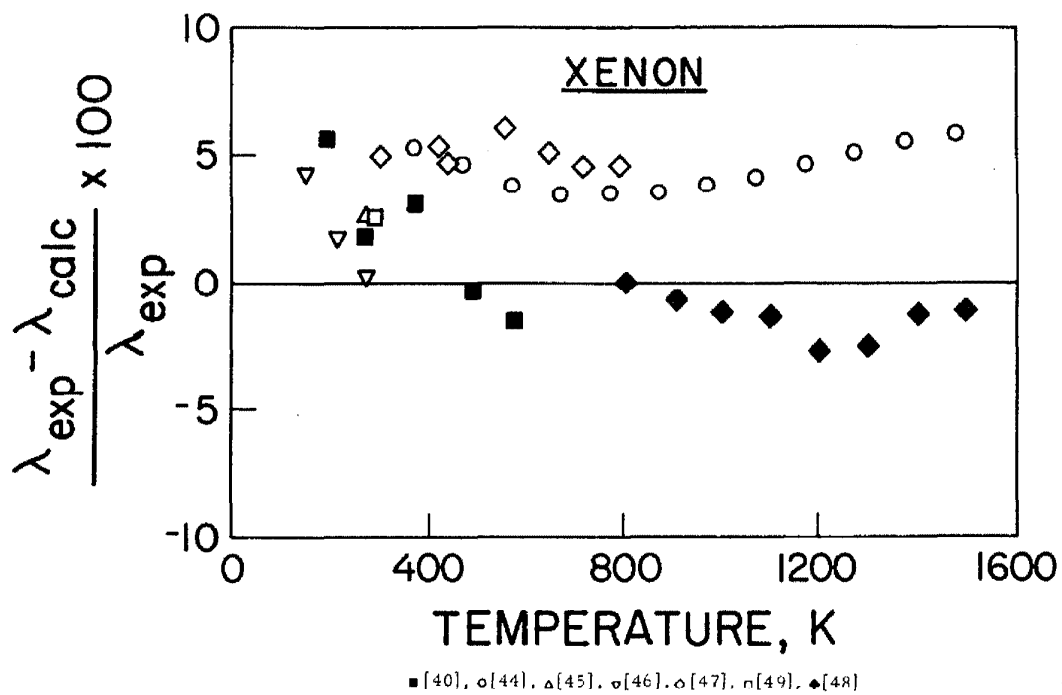


FIGURE 6. Deviation curve for the thermal conductivity of xenon. Theoretical values calculated from equation (7) with parameters given in table 2.

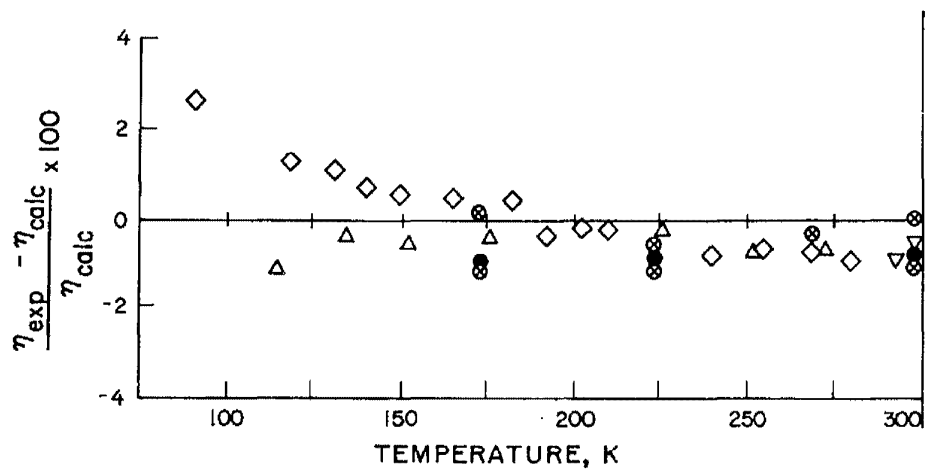


FIGURE 7. Comparison between several sets of viscosity data for argon, including that recently measured by Haynes (crossed circles). The base line was calculated from the 11-6-8 potential as in figure 1 (key as in fig. 1).

low temperatures. A further accuracy assessment can be made by examining such data in more detail.

Let us consider argon only because much of the data for all three gases, argon, krypton, and xenon, were obtained from the same sources. Figure 7 expands figure 1 and plots deviations between experimental viscosity coefficients and the tabulated values. Five data sets are represented: Kestin [12], Johnston [22], Clark [14], Gracki [23], and the very recent data of Haynes [27]. The figure indicates that these data sets lie within about one percent of each other above 120 K and are within one percent of our correlation; on the basis of an examination of these experimental papers, we assigned accuracies to the data as follows: [12], 0.5 percent; [22] and [27], 2 percent; [14] and [23], 1 percent. Moreover, the sets represent three different experimental procedures, the oscillating disc [12, 22], the capillary flow [14, 23], and the oscillating crystal [27]. We therefore conclude that one percent is a fair estimate of uncertainty for our representation.

It could be argued that a one percent estimate is too conservative for the data around room temperature and that our correlated values are too high. At these temperatures, extremely precise results have been reported; Kestin, et al. [12b], for example, quote a precision of their experimental viscosity coefficient at 298.15 of 0.2 percent. (The accuracy of this datum point is not necessarily so well defined.)

However, by examining data for a wide temperature range for all three gases, shown in figures 1-3 and 7 (and figures 4-6 for the thermal conductivity coefficient) we suggest that an overall accuracy estimate of ± 1 percent for the viscosity coefficient in the temperature range 100-1000 K properly reflects the accuracy in the data and that our tables, for both transport coefficients, reflect this estimate. Giving equal weight to the low temperature data of references [14] and [22] and to the high temperature data of references [15] and [13, 16, 17], the estimate could be increased to ± 2 percent below 100 K and to $\pm 1\frac{1}{4}$ percent above 1000 K.

2. The second approach supplements the first. In fact, it has been directly applied because second virial coefficient data were required to assist in the selection of $m-6-8$ potential parameters used to generate the viscosity and thermal conductivity coefficients. Figures 1-3 reveal that the fits of experimental virial coefficients are excellent. Even though the $m-6-8$ is not, of course, an exact representation of the intermolecular interactions for the rare gases, and the virial data clearly are not error free, one has to conclude from figures 1-3 that the viscosity coefficients and second virial coefficients are consistent.

It has been discussed in reference [55] that the $m-6-8$ potential also leads to a satisfactory and consistent representation of the self-diffusion coefficient and the isotopic thermal diffusion factor for argon, krypton, and xenon. Given the parameters of table 2, comparisons between theory and experiment for these properties

are presented here. The statistical mechanical equations are:

Thermal Diffusion Factor, α_0

Kihara's [55] equation for α_0 is

$$\alpha_0 = \alpha'_0 (1 + \delta), \quad (10)$$

where

$$\alpha'_0 = \frac{15 (6C^* - 5) (2A^* + 5)}{2A^* (16A^* - 12B^* + 55)}, \quad (11)$$

with δ given by

$$\begin{aligned} \delta = & \frac{I^*}{9} \left\{ \frac{2A^*}{\left(\frac{35}{4}\right) + 7A^* + 4F^*} \right. \\ & \times \left[H^* + \frac{1}{2} \left(\frac{7(5 - 6C^*) + A^* I^*}{5 + 2A^*} \right) \right. \\ & \times \left. \left(\frac{\left(\frac{35}{8}\right) + 28A^* - 6F^*}{21A^*} \right) \right] \\ & - \frac{5}{7} \left[H^* - \frac{7}{5} \left(\frac{5 - 6C^*}{5 + 2A^*} \right) - \frac{3I^*}{10} \right] \}, \end{aligned} \quad (12)$$

where

$$I^* = 7 - 8E^*, \quad (13)$$

and

$$H^* = \frac{\left(\frac{35}{4} - 3B^* - 6C^*\right)}{5 - 6C^*}. \quad (14)$$

The potential function enters into the equation for α_0 through the ratios of collision integrals A^* , B^* , C^* , E^* , and F^* :

$$\begin{aligned} A^* &= \Omega^{(2,2)*}/\Omega^{(1,1)*}, \\ B^* &= (5\Omega^{(1,2)*} - 4\Omega^{(1,3)*})/\Omega^{(1,1)*}, \\ C^* &= \Omega^{(1,2)*}/\Omega^{(1,1)*}, \\ E^* &= \Omega^{(2,3)*}/\Omega^{(2,2)*}, \\ F^* &= \Omega^{(3,3)*}/\Omega^{(1,1)*}. \end{aligned} \quad (15)$$

Self-diffusion Coefficient, D

The equation for the self-diffusion coefficient is:

$$\rho D = \frac{5}{8} \frac{(\pi m kT)^{1/2}}{\pi \sigma^2 \Omega^{(1,1)*}} f_D, \quad (16)$$

where

$$f_D = 1 + (6C^* - 5)^2/(16A^* + 40), \quad (17)$$

and ρ is the mass density.

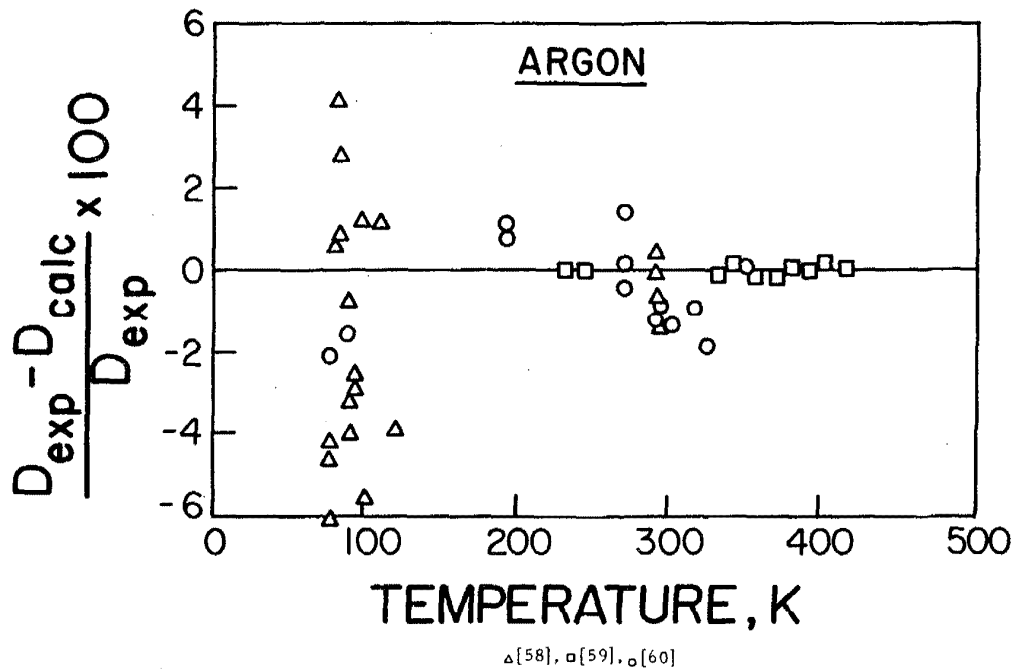


FIGURE 8. Comparison between experimental self-diffusion coefficients of argon and to theoretical values determined from equation (16) with the $m-6-8$ potential using the same parameters required by the viscosity and second virial coefficients. Note: the data from [59] are relative to D at 298.15 K. We used the calculated value for this reference point.

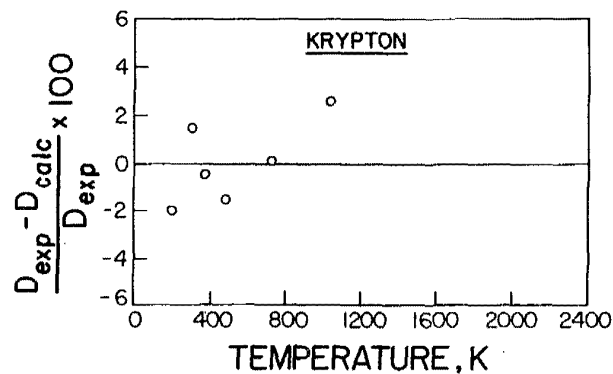


FIGURE 9. Deviation curve for the self-diffusion coefficient of krypton from equation (16) with the parameters given in table 2, experiment from [60].

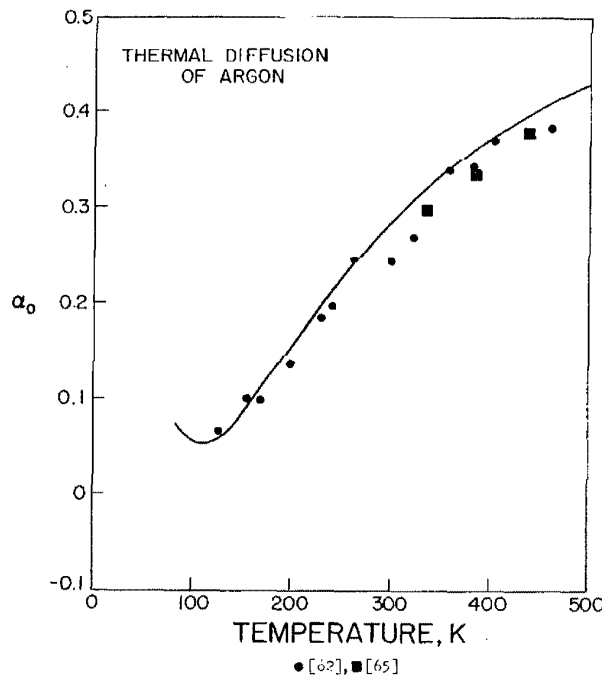


FIGURE 10. Experimental and theoretical (equation (10)) thermal diffusion factors for argon. We use the same $m-6-8$ potential as for the other transport coefficients.

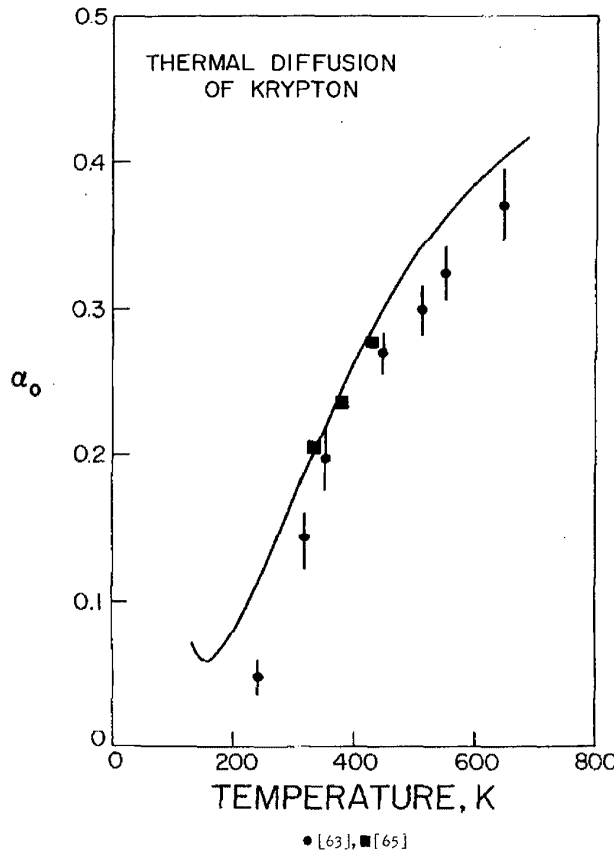


FIGURE 11. The isotopic thermal diffusion factor for krypton calculated from equation (10), using parameters given in table 2, compared to experiment.

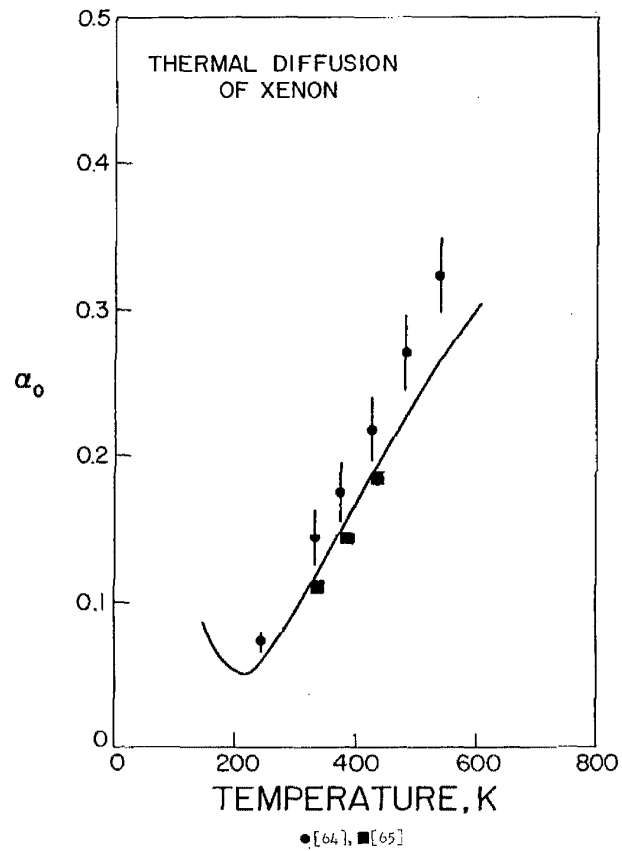


FIGURE 12. The isotopic thermal diffusion factor for xenon calculated from equation (10), using parameter given in table 2, compared to experiment.

Diffusion coefficients were calculated for argon and krypton from equation (16) using the parameters listed in table 2. Comparisons between calculated values and data from references [58-61] are shown in figures 8 and 9. Isotopic thermal diffusion factors were obtained from equation (10) for argon, krypton, and xenon and compared to data from references [62-65] in figures 10-12.

To summarize, figures 1-3 and 8-12, in conjunction with the experimental considerations, reinforce the conclusion that the tabulated viscosity and thermal conductivity coefficients are consistent with other properties of the gases, are free from serious systematic errors, and that the accuracy estimate quoted above is reasonable. In fact, based on the consistent representation of the virial coefficients, the diffusion coefficients and the isotopic thermal diffusion factor at low temperatures, the previous estimate of ± 2 percent accuracy for the tabulated viscosity and thermal conductivity coefficients may be too high. Accordingly, we lower the estimate to ± 1 percent for temperatures between 80 and 100 K.

Unfortunately, the figures 1-3 and 8-12, do not properly resolve the discrepancy between the two sets of viscosity data, for all gases, above 1000 K. An accuracy assignment of $\pm 1\frac{3}{4}$ percent, based on the difference between these data, is therefore given to our tabulated values for temperatures between 1000 and 2000 K.

4.2. The Potential Function and Extrapolation of the Tables

Although the $m-6-8$ is a very practical model to insert into statistical mechanical equations, it is not exact. We have discussed the various model potentials—particularly those for argon—that have been proposed [54, 55] and indicated how they can represent data on the one hand, and how they are compatible with known information on the nature of intermolecular interactions on the other hand. It seems that for “normal” temperatures—a reduced temperature range of $0.5 \leq T^* \leq 20$, say—the $m-6-8$ potential is completely adequate when required to represent macroscopic properties. Outside this range, however, intermolecular interactions depend strongly on the nature of the potential at small intermolecular separations (high temperatures) or at very large separations (low temperatures), and we have previously discussed that the form of the $m-6-8$ is insufficiently flexible to represent intermolecular interactions at these extremes. For example, it is shown in reference [55] that the potential is too hard at small r , and that numerical values of the dispersion coefficients (the coefficients of the $1/r^6$ and $1/r^8$ terms of equation (8)) do not agree with independent quantum mechanical estimates.

However, it is not yet clear how a “normal” temperature range can be properly defined, so one can only estimate at what temperatures the $m-6-8$ will fail to reproduce data. The problem is compounded because

the available data for gases tend to become progressively more imprecise at very high or at very low temperatures. Our estimate is that the procedure presented here could be used to calculate transport properties for temperatures up to about 4000 K. An estimate for a lower limit would be about the triple point temperature. In any case, these limits are somewhat academic because ionization would occur at high temperatures, and the gas can only exist at an extremely low pressure at very low temperatures.

5. Conclusion

We have generated tables for the dilute gas viscosity and thermal conductivity coefficients for argon, krypton, and xenon using the $m-6-8$ potential with selected experimental data. On the basis of an analysis of the input data and from the results obtained when the $m-6-8$ potential, with parameters chosen to correlate the viscosity coefficients, was inserted into statistical mechanical equations for other properties, we place an estimate of uncertainty of one percent in the tabulated values for temperatures up to 1000 K. The uncertainty estimate is set at one and three quarters percent for temperatures between 1000 and 2000 K. A feature of this viscosity and thermal conductivity correlation is that these coefficients are consistent with other macroscopic properties of the dilute and moderately dense gas.

We are most grateful for the cooperation and help given by the authors of many of the experimental papers listed. We are particularly grateful to Professor J. Kestin of Brown University, Professor E. B. Smith of Oxford, Dr. G. P. Flynn of Brown and MIT, Dr. W. M. Haynes of NBS-Boulder, and Drs. B. B. McInteer and F. Guevara of the Los Alamos Scientific Laboratory who gave valuable comments and, in many cases, allowed us to examine their data prior to publication. The continuing cooperation and advice of Dr. Max Klein of NBS-Washington is also gratefully acknowledged. This work was supported by the Office of Standard Reference Data.

6. References

- [1] Bruges, E. A. and Whitelaw, J. H., "Proc. 4th Symp. Thermophys. Prop." ASME, New York (1968), p. 462.
- [2] Barr, G., "A Monograph of Viscosity," Oxford University Press, London (1931).
- [3] Tye, R. P., Ed. "Thermal Conductivity," Academic Press, New York (1969).
- [4] Golubev, I. F., "Viscosity of Gases and Gas Mixtures," Translated (1970) by the Israel Program for Scientific Translations, U.S. Dept. of the Interior and the National Science Foundation, Washington, D.C.
- [5] Vargaftik, N. B., Filippov, L. P., Tarzimanov, A. A., and Iurchak, R. P., "Thermal Conductivity of Gases and Liquids," Moscow (1970).
- [6] Tsvetberg, N. V., "Thermal Conductivity of Gases and Liquids", M.I.T. Press, Cambridge, Mass. (1965).
- [7] See for example, Kestin, J., Leidenfrost, W., and Liu, C. Y., Z.

TABLE 3. Viscosity and thermal conductivity coefficients of argon—Continued

TEMPERATURE K	VISCOSITY G/CM-S $10^3 \eta$	THERMAL CONDUCTIVITY W/CM-K $10^3 \lambda$	TEMPERATURE K	VISCOSITY G/CM-S $10^3 \eta$	THERMAL CONDUCTIVITY W/CM-K $10^3 \lambda$
1660	0.7762	0.6084	1910	0.8500	0.6662
1670	0.7793	0.6107	1920	0.8529	0.6685
1680	0.7823	0.6131	1930	0.8558	0.6707
1690	0.7853	0.6155	1940	0.8586	0.6730
1700	0.7883	0.6178	1950	0.8615	0.6752
			1960	0.8644	0.6775
1710	0.7912	0.6201	1970	0.8672	0.6797
1720	0.7943	0.6225	1980	0.8700	0.6819
1730	0.7973	0.6249	1990	0.8729	0.6842
1740	0.8003	0.6272	2000	0.8757	0.6864
1750	0.8032	0.6296			
1760	0.8062	0.6319			
1770	0.8092	0.6342			
1780	0.8121	0.6365			
1790	0.8151	0.6388			
1800	0.8180	0.6412			
1810	0.8210	0.6435			
1820	0.8239	0.6458			
1830	0.8268	0.6481			
1840	0.8297	0.6503			
1850	0.8326	0.6526			
1860	0.8355	0.6549			
1870	0.8384	0.6571			
1880	0.8414	0.6595			
1890	0.8443	0.6617			
1900	0.8472	0.6640			

TABLE 4. Viscosity and thermal conductivity coefficients of krypton—Continued

Y TEMPERATURE K	VISCOSITY G/CM-S $10^3 \eta$	THERMAL CONDUCTIVITY W/CM-K $10^3 \lambda$	TEMPERATURE K	VISCOSITY G/CM-S $10^3 \eta$	THERMAL CONDUCTIVITY W/CM-K $10^3 \lambda$
1660	0.9391	0.3508	1910	1.0298	0.3847
1670	0.9428	0.3522	1920	1.0333	0.3860
1680	0.9466	0.3536	1930	1.0368	0.3873
1690	0.9503	0.3550	1940	1.0403	0.3886
1700	0.9540	0.3563	1950	1.0438	0.3899
			1960	1.0473	0.3912
1710	0.9577	0.3577	1970	1.0508	0.3925
1720	0.9614	0.3591	1980	1.0542	0.3938
1730	0.9650	0.3605	1990	1.0578	0.3952
1740	0.9687	0.3618	2000	1.0612	0.3965
1750	0.9723	0.3632			
1760	0.9759	0.3646			
1770	0.9796	0.3659			
1780	0.9833	0.3673			
1790	0.9869	0.3687			
1800	0.9905	0.3700			
1810	0.9941	0.3714			
1820	0.9977	0.3727			
1830	1.0013	0.3741			
1840	1.0049	0.3754			
1850	1.0084	0.3767			
1860	1.0120	0.3780			
1870	1.0155	0.3794			
1880	1.0192	0.3807			
1890	1.0227	0.3821			
1900	1.0262	0.3834			

TABLE 5. Viscosity and thermal conductivity coefficients of xenon—Continued

TEMPERATURE K	VISCOSITY G/CM-S $10^3 \eta$	THERMAL CONDUCTIVITY W/CM-K $10^3 \lambda$	TEMPERATURE K	VISCOSITY G/CM-S $10^3 \eta$	THERMAL CONDUCTIVITY W/CM-K $10^3 \lambda$
1660	0.9331	0.2224	1910	1.0256	0.2445
1670	0.9369	0.2233	1920	1.0292	0.2453
1680	0.9407	0.2242	1930	1.0327	0.2462
1690	0.9445	0.2251	1940	1.0363	0.2470
1700	0.9483	0.2260	1950	1.0398	0.2478
			1960	1.0435	0.2487
1710	0.9521	0.2269	1970	1.0470	0.2496
1720	0.9558	0.2278	1980	1.0506	0.2504
1730	0.9596	0.2287	1990	1.0541	0.2513
1740	0.9633	0.2296	2000	1.0576	0.2521
1750	0.9671	0.2305			
1760	0.9708	0.2314			
1770	0.9745	0.2323			
1780	0.9782	0.2331			
1790	0.9818	0.2340			
1800	0.9855	0.2349			
1810	0.9893	0.2358			
1820	0.9929	0.2367			
1830	0.9966	0.2375			
1840	1.0003	0.2384			
1850	1.0039	0.2393			
1860	1.0075	0.2401			
1870	1.0112	0.2410			
1880	1.0148	0.2419			
1890	1.0184	0.2427			
1900	1.0220	0.2436			

